



A High Gain Bidirectional Buck Converter Using Coupled Inductor

Megha.C¹, S.Priya²

Department of EEE, NSS College of Engineering, Palakkad, Kerala India¹

Professor, Department of EEE, NSS College of Engineering, Palakkad, Kerala, India²

Abstract: The paper introduces, a high step-down bidirectional converter, utilizing one coupled inductor and two energy-transferring capacitors, is presented. The capacitor connected between input voltage and coupled inductor plays a role to step down the input voltage. The corresponding voltage conversion ratio is lower than traditional buck converter and tapped inductor buck converter. Moreover, the output voltage varies with the duty cycle linearly, making control easier. The output voltage not only depends on duty cycle but on number of turns in the coupled inductor. Furthermore, the leakage inductance energy can be recycled thereby reducing the switching losses and thus the efficiency can be improved.

Keywords: Step-down converter, coupled inductor, duty cycle, number of turns.

I. INTRODUCTION

Step-down converters are widely used in digital circuit power systems, which needs lower input voltages. In general, a 48 V voltage source generated from the AC-DC converter is used for communication systems in the network communication room. However, for the device which needs an input voltage of 3.3 V or less, an extremely low duty cycle is necessary for the buck converter if the input voltage is 48 V, thereby causing the control design to be tough and the accompanying power loss to be relatively high. Up to now, the two-stage step-down structure has been widely employed in the applications which need much lower voltage conversion ratio. For example, in order to power the CPU, the RAM and the hard disk, the first stage transfers 48 to 12 V to power the point of load (POL), and then the POL, called the second stage, transfers 12 to 3.3, 2.5, 1.8, 1.5, 1.2 or 1 V.

This paper presents a high step-down converter, which utilizes one coupled inductor, two energy-transferring capacitors with small capacitances. Furthermore, the voltage conversion ratio of this converter is much lower than that of the traditional buck converter. Above all, its output voltage varies with the duty cycle linearly. In addition, the proposed high step-down converter can be operated in the step-up mode. Therefore, the proposed converter can be used in the energy harvesting applications, such as thermo-electric generation system, which can convert heat energy into electricity.

II. PROPOSED CONVETER MODEL

Fig. 1 shows the proposed bidirectional converter, which contains four switches Q_1 , Q_2 , Q_3 , and Q_4 , two energy-transferring capacitors C_1 and C_2 , and one coupled

inductor composed of the primary winding N_1 and the secondary winding N_2 . More-over, Q_1 and Q_3 are driven simultaneously, whereas Q_2 and Q_4 are driven simultaneously. Although there are four switches in this circuit, only two half-gate drivers are required to drive them. In addition, the high-voltage side is denoted by V_H , and the low-voltage side is signified by V_L .

The equivalent circuit of the proposed converter is shown in Fig. 2. The coupled inductor is modelled as an ideal transformer with the primary winding N_1 and the secondary winding N_2 , a magnetizing inductor L_m connected in parallel with the N_1 winding, and a leakage inductor L_{lk} . Besides, in order to make the analysis of the proposed converter easier, there are some assumptions to be made as follows:

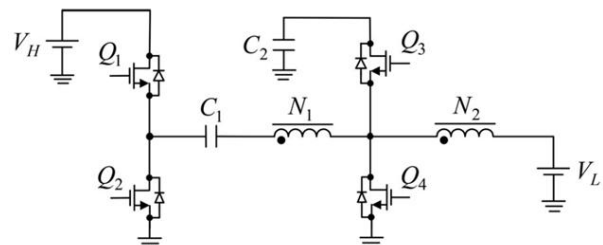


Fig. 1 Proposed Bidirectional Converter

- 1) The proposed converter operates in the positive current region, that is, the current flowing through the magnetizing inductor L_m is always positive;
- 2) All the switches and diodes are assumed to be ideal components;
- 3) The values of all the capacitors are large enough such that the voltages across them are kept constant at some values.



The following analysis contains the operating principles, voltage gains, and boundary conditions of the magnetizing inductor in step-down and step-up modes, influence of leakage inductance, and performance comparison with different step-down converters. In addition, the currents flowing through $Q_1, Q_2, Q_3, Q_4, C_1, C_2, L_{lk}, N_1, N_2,$ and L_m are signified by $i_{DS1}, i_{DS2}, i_{DS3}, i_{DS4}, i_{C1}, i_{C2}, i_{lk}, i_{N1}, i_{N2},$ and i_{Lm} , respectively. Furthermore, the voltage across L_m or the voltage across the N_1 winding is signified by v_{Lm} , the voltage across the N_2 winding is represented by v_{N2} , and the voltages across C_1 and C_2 are indicated by V_{C1} and V_{C2} .

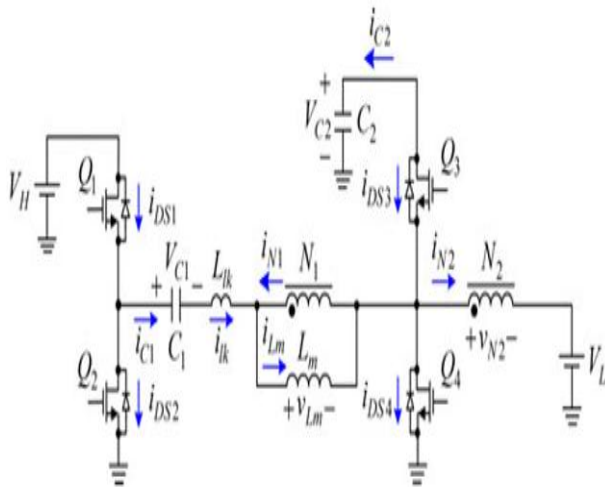


Fig. 2 Equivalent Circuit of Proposed Model

A. Step-Down Mode

For the proposed converter operating in the positive current region, there are ten operating states, to be described as follows. Fig. 3 shows the illustrated waveforms over one switching period. It is noted that the current i_{N1} is the same as the current i_{N2} except that there is a difference in amplitude between the two.

1. State 1 [t_0, t_1]: As shown in Fig. 4(a), the switches Q_1 and Q_3 are turned ON, but the switches Q_2 and Q_4 are turned OFF. During this state, a positive voltage is imposed on the magnetizing inductor L_m and the leakage inductor L_{lk} , making both L_m and L_{lk} magnetized. In the meantime, the capacitor C_1 is charged, and the currents in the N_1 winding and the capacitor C_2 , i.e., i_{N1} and i_{C2} , are decreasing slowly, providing energy to the load. This state comes to an end once i_{C2} reaches zero at t_1 .

2. State 2 [t_1, t_2]: As shown in Fig. 4(b), the switches Q_1 and Q_3 keep turned ON, but the switches Q_2 and Q_4 keep turned OFF. During this state, the capacitor C_2 is charged, so the current i_{C2} is increasing continuously. Meanwhile, the current i_{N1} is continuously decreasing. This mode ends when i_{N1} drops to zero at t_2 .

3. State 3 [t_2, t_3]: As shown in Fig. 4(c), the switches Q_1 and Q_3 still keep turned ON, but the switches Q_2 and Q_4

still keep turned OFF. During this state, the currents i_{lk} and i_{Lm} keep increasing, and the current i_{N2} is also increasing in the opposite direction. As a result, the current i_{C2} is the sum of i_{lk} and $-i_{N2}$. This state ends as Q_1 and Q_3 are turned OFF at t_3 .

4. State 4 [t_3, t_4]: As shown in Fig. 4(d), the switches Q_1 and Q_3 become turned OFF, and the switches Q_2 and Q_4 keep turned OFF. During this blanking time period, the body diodes of Q_2 and Q_3 are forward biased by the leakage inductance current i_{lk} . Meanwhile, the voltage $(V_{C2} - V_L) \times N_1 / N_2$ is imposed on the magnetizing inductor L_m , causing L_m to be continuously magnetized, and the current i_{lk} is gradually declining. This state comes to an end while Q_2 and Q_4 become turned ON at t_4 .

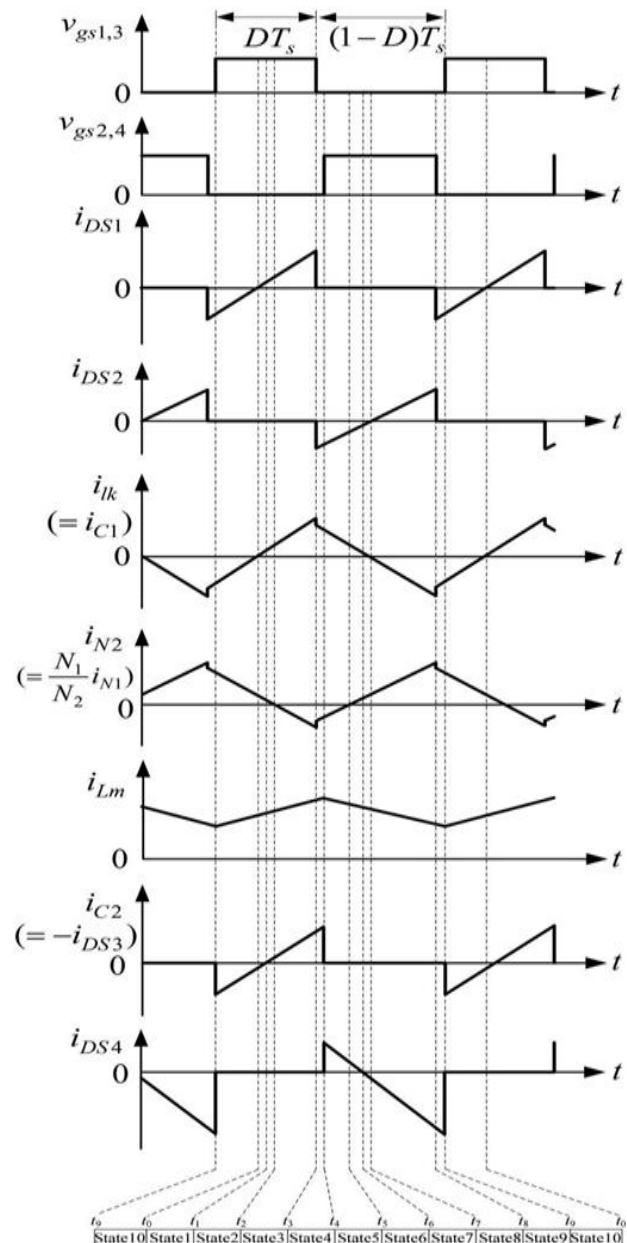


Fig. 3 Illustrated Waveform for Step-Down Mode

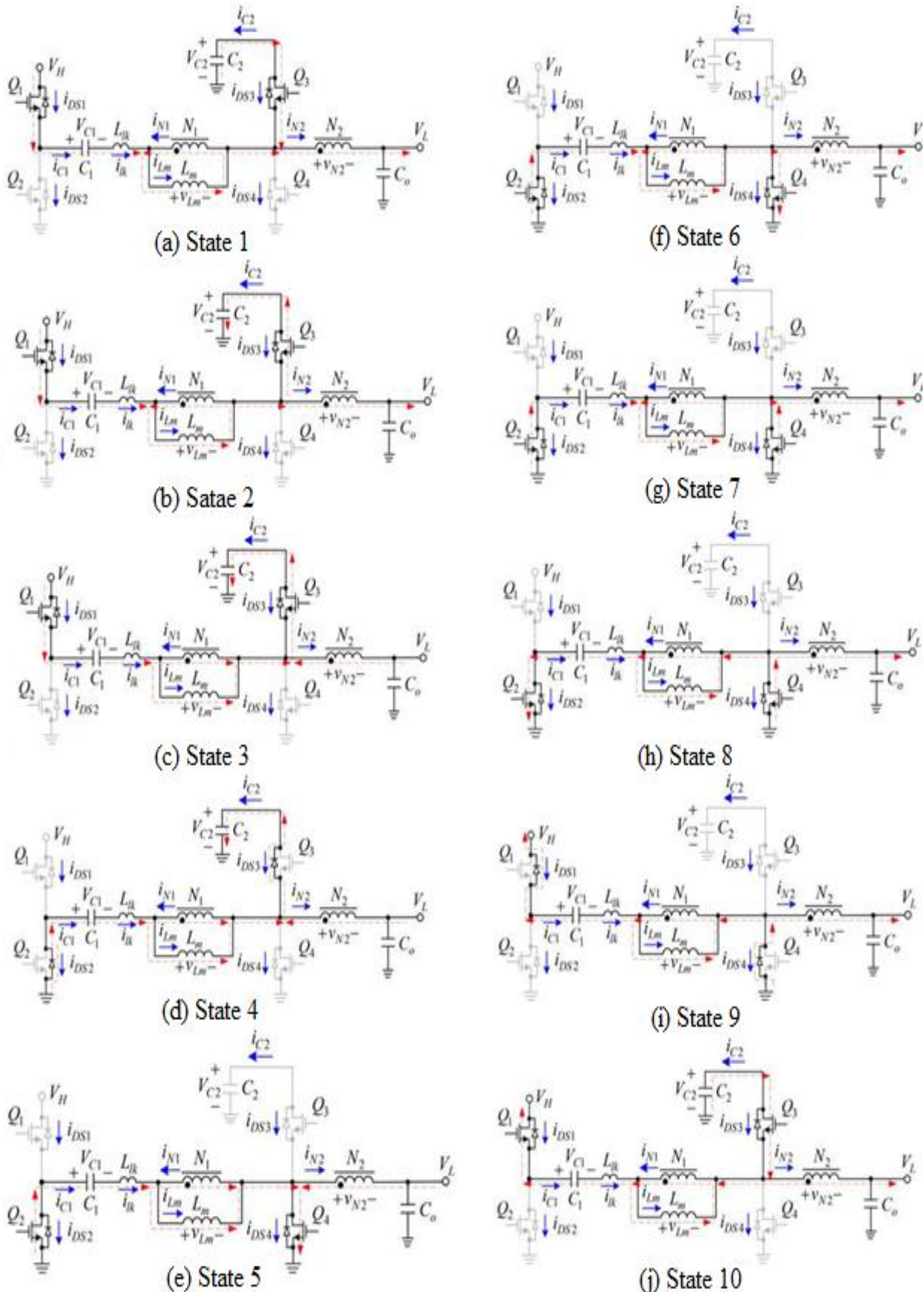


Fig. 4 Power Flow Path over One Switching Period in Step-Down Mode

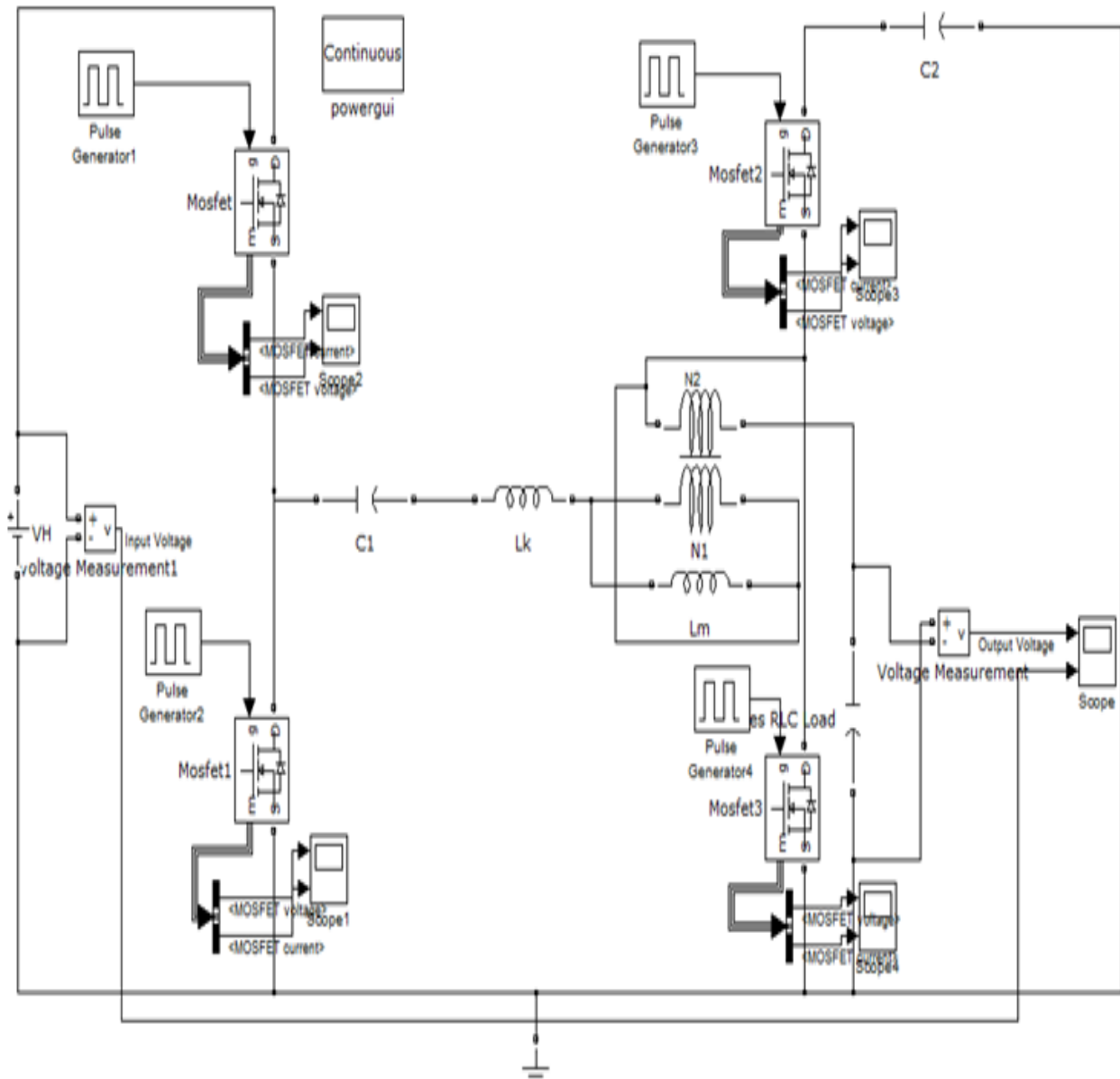


Fig. 6 Simulation Diagram

5. State 5 [t_4, t_5]: As shown in Fig. 4(e), the switches Q_1 and Q_3 keep turned OFF, but the switches Q_2 and Q_4 become turned ON. Since there is a current flowing through the body diode of Q_2 before state 5 begins, Q_2 can achieve ZVS turn-on. Meanwhile, the voltage $-V_{C1}$ is imposed on the magnetizing inductor L_m , thereby causing L_m to be demagnetized and the current i_{lk} is gradually declining. The current i_{N2} is decreasing until it reaches zero at t_5 , and this state ends.

6. State 6 [t_5, t_6]: As shown in Fig. 4(f), the switches Q_1 and Q_3 still keep turned OFF, and Q_2 and Q_4 still keep turned ON. During this state, the current i_{lk} is decreasing and the current i_{N2} is increasing. L_m keeps demagnetized. As soon as i_{lk} is smaller than i_{N2} , the current i_{DS4} will change the current direction. As i_{DS4} drops to zero, this state ends at t_6 .

7. State 7 [t_6, t_7]: As shown in Fig. 4(g), the switches Q_1 and Q_3 are still turned OFF, but Q_2 and Q_4 are still turned ON. During this state, the magnetizing inductor L_m still keeps demagnetized, the current i_{lk} is still decreasing, the current i_{N2} is still increasing, and the current i_{DS4} is increasing in the opposite direction. This state comes to an end once i_{lk} reaches zero at t_7 .

8. State 8 [t_7, t_8]: As shown in Fig. 4(h), the switches Q_1 and Q_3 are still in the turn-off state, but Q_2 and Q_4 are still in the turn-on state.

During this state, the magnetizing inductor L_m still keeps demagnetized, the current i_{lk} is increasing in the opposite direction, the current i_{N2} is still increasing, and the current i_{DS4} is increasing in the opposite direction. This state ends when Q_2 and Q_4 are turned OFF at t_8 .



9. State 9 [t₈, t₉]: As shown in Fig. 4(i), the switches Q₁ and Q₃ still keep turned OFF, and the switches Q₂ and Q₄ become turned OFF. During this blanking time period, the body diodes of Q₁ and Q₄ are forward biased by the current i_{lk}, and also, the magnetizing inductor L_m keeps demagnetized. Meanwhile, the leakage inductor L_{lk} is demagnetized, and i_{N2} is decreasing. This state comes to an end when Q₁ and Q₃ are turned ON at t₉. Meanwhile, the leakage inductor L_{lk} is demagnetized, and i_{N2} is decreasing. This state comes to an end when Q₁ and Q₃ are turned ON at t₉.

10. State 10 [t₉, t₀]: As shown in Fig. 4(j), the switches Q₂ and Q₄ keep turned OFF, but the switches Q₁ and Q₃ become turned ON. Before the state 10 begins, there is a current flowing through the body diode of Q₁, and hence, Q₁ can be turned ON with ZVS.

On the other hand, the leakage inductor L_{lk} is still demagnetized, and C₂ is discharging energy to the load. This state ends when the current i_{lk} reaches zero at t₀, and the next cycle is repeated.

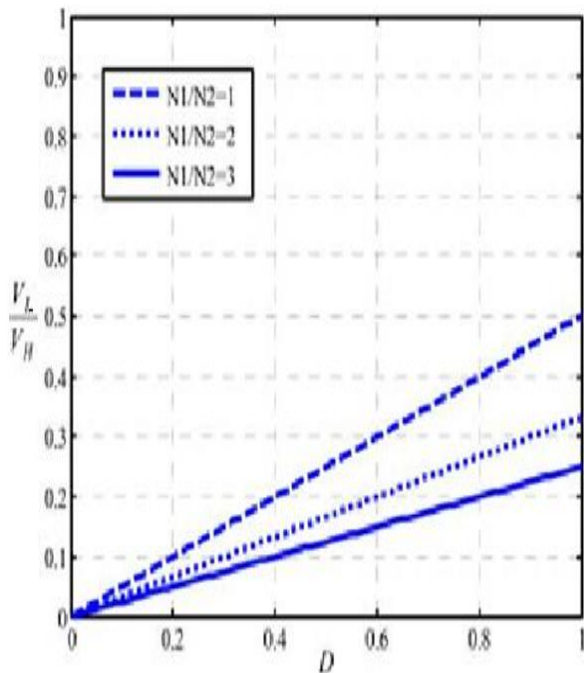


Fig. 5 Voltage Gain versus Duty Cycle with Different Values of Turns Ratio

B. ZVS Achievements

From the above analyses of the step-down mode, the ZVS states can be summarized as below

TABLE I ZVS ACHIEVEMENT SUMMARIZATION

Switch Mode	Q ₁	Q ₂	Q ₃	Q ₄
Step-Down	ZVS turn-on	ZVS turn-on	ZVS turn-off	ZVS turn-off

C. Voltage Gain in Step-Down Mode

To attain the voltages across C₁ and C₂, and the voltage gain, only states 2 and 5 as shown in Fig. 4(b) and (e) are considered herein with the blanking times and the leakage inductor L_{lk} ignored. From state 5, V_{C1} can be found to be

$$V_{C1} = V_L \times \frac{N_1}{N_2} = -v_{Lm} \tag{1}$$

Furthermore, from state 2, V_{C2} can be described to be

$$V_{C2} = V_L + (V_H - V_{C1} - V_L) \cdot \frac{N_2}{N_1+N_2} \tag{2}$$

In addition, by applying the voltage-second balance principle to L_m over one switching period, the following equation can be obtained to be

$$D \cdot (V_H - V_{C1} - V_L) \cdot \frac{N_1}{N_1+N_2} = (1 - D) \cdot V_L \cdot \frac{N_1}{N_2} \tag{3}$$

The corresponding voltage gain can be expressed by

$$\frac{V_L}{V_H} = D \cdot \frac{N_2}{N_1+N_2} \tag{4}$$

It can be seen that the voltage gain of the proposed converter can be adjusted not only by the duty cycle but also by the primary and secondary turns. Fig. 5 shows the curves of voltage gain versus duty cycle of the proposed converter, considering different values of turns ratio.

D. Performance Comparison with Different Step-Down Converters

The proposed converter is compared with four step-down type converters as shown in Table II. There are traditional buck converter, two-stage buck converter, tapped-inductor buck converter, full-bridge converter, and the proposed converter.

For the voltage gain, under the same duty cycle and turns ratio, the proposed converter has a higher step-down value, and the voltage stresses are smaller than the tapped-inductor buck converter, which also uses a coupled inductor. Moreover, the number of components of the proposed converter is lower than that of the full-bridge converter.

III.SIMULATION

The simulation for the prototype was developed using MATLAB/Simulink package as in Fig.6. In this model duty ratio is taken to be 28% and turns ratio to 1:3. Other parameters are L_m=86mH, L_{lk} = 1.5mH, V_H = 48 V, switching frequency f_s = 100 kHz

Fig. 7 shows the output of simulated model. The simulated output has a slight deviation from the expected output due to the variation in parameters.



TABLE II COMPARISON OF DIFFERENT STEP-DOWN CONVERTERS

Converter	Traditional Buck	Two-Stage Buck	Tapped Inductor Buck	Full Bridge	Proposed
Voltage gain	D	D^2	$\frac{D}{1 + \frac{N_1}{N_2}(1 - D)}$	$D \frac{N_2}{N_1}$	$D \frac{N_2}{N_1 + N_2}$
Number of switch	1	2	1	4	4
Number of diode	1	2	1	4	0
Number of coupled inductor or transformer	0	0	1	1	1
Number of capacitor	1	2	1	2	3
Number of output inductor	1	2	0	1	0
Switch voltage stress	$V_{ds1} = V_{in}$	$V_{ds1} = V_{in}$ $V_{ds2} = DV_{in}$	$V_{ds1} = \frac{1 + \frac{N_1}{N_2}}{D} V_o$	$V_{ds1} = V_{ds2} = V_{ds3} = V_{ds4}$	$V_{ds1} = V_{ds2}$ $V_{ds3} = V_{ds4}$
Isolation	NO	NO	NO	YES	NO

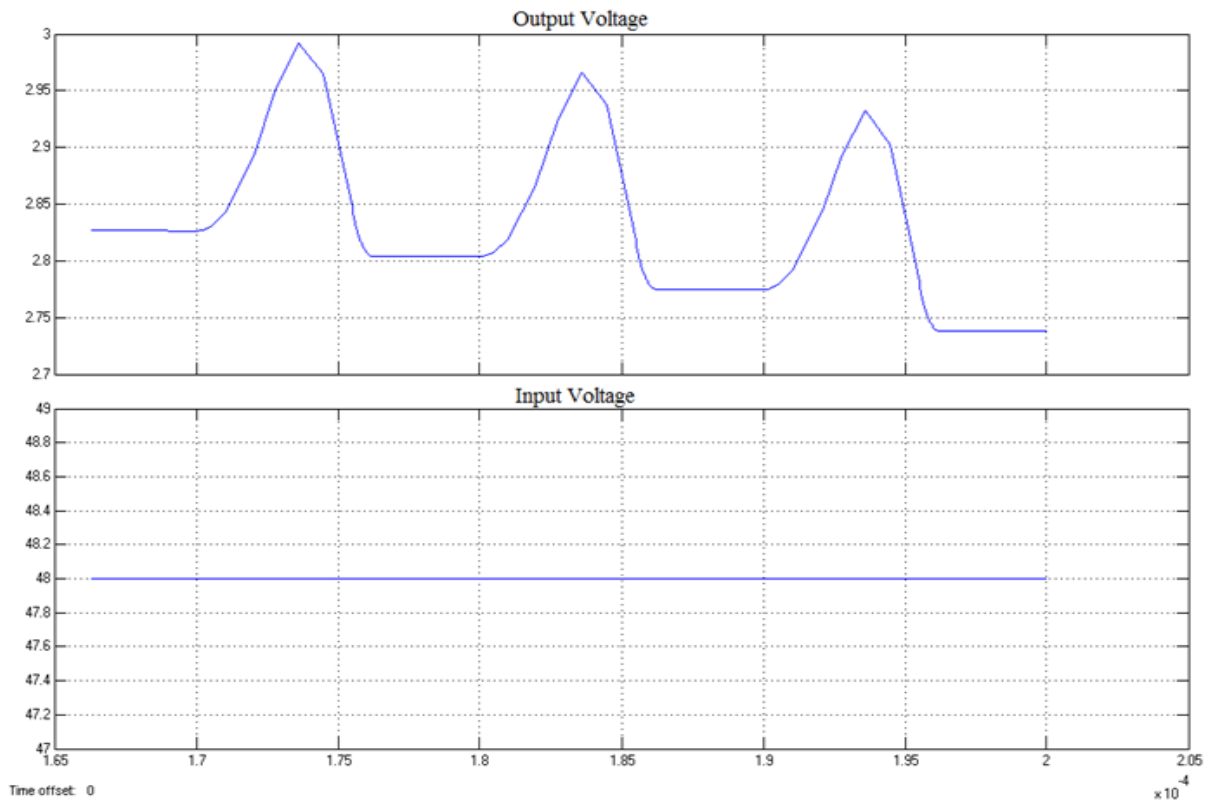


Fig . 7 Output Waveform of Simulated Model

IV. CONCLUSION

First of all, a high step-down bidirectional converter, utilizing a coupled inductor and two energy-transferring capacitors is presented. In the step-down mode, the corresponding voltage conversion ratio is much lower than that of the traditional buck converter. Furthermore, the output voltage varies with the duty cycle linearly. In the step-up mode, the voltage gain is much higher than that of the traditional boost converter. Moreover, in the step-down

mode, the switches Q_1 and Q_2 can achieve ZVS turn-on and the switches Q_3 and Q_4 can achieve ZVS turn-off, whereas in the step-up mode, the switches Q_1 and Q_2 can achieve ZVS turn-off and the switches Q_3 and Q_4 can achieve ZVS turn-on. The leakage inductance energy can be recycled. In addition, the four switches can be driven by using two half-bridge gate drivers, without any isolated gate drivers. The proposed converter can be operated in



the step-up mode; thus, it can be used in the energy-harvesting applications, such as thermoelectric generation system. Since the proposed converter can be operated in a bidirectional way, it can also be used in the burn-in test applications. To sum up, the structure of the proposed converter is quite simple and very suitable for different applications in the industry.

REFERENCES

- [1] Y. Ren, M. Xu, K. Yao, Y. Meng, F. C. Lee, J. Guo, and Y. Ren, "Two-stage approach for 12 V VR," in Proc. IEEE Appl. Power Electron. Conf., 2004, vol. 2, pp. 1306–1312.
- [2] Y. Ren, M. Xu, K. Yao, and F. C. Lee, "Two-stage 48 V power pod exploration for 64-bit microprocessor," in Proc. IEEE Appl. Power Electron. Conf., 2003, vol. 1, pp. 426–431.
- [3] K. I. Hwu and Y. T. Yau, "Resonant voltage divider with bidirectional operation and startup considered," IEEE Trans. Power Electron., vol. 27, no. 4, pp. 1996–2006, Apr. 2012.
- [4] W. Li, J. Xiao, J. Wu, J. Liu, and X. He, "Application summarization of coupled Inductors in DC-DC converters," in Proc. IEEE Appl. Power Electron. Conf., 2009, pp. 1487–1492.
- [5] J. A. B. Vieira and A.M. Mota, "Thermoelectric generator using water gas heater energy for battery charging," in Proc. IEEE Conf. Control Appl. Intell. Control, 2009, pp. 1477–1482.
- [6] D. A. Grant, Y. Darroman, and J. Suter, "Synthesis of tapped-inductor switched-mode converters," IEEE Trans. Power Electron., vol. 22, no. 5, pp. 1964–1969, Sep. 2007.
- [7] M. Batarseh, X. Wang, and I. Batarseh, "Non-isolated half bridge buck based converter for VRM application," in Proc. IEEE Power Electron. Spec. Conf., 2007, pp. 2393–2398.
- [8] K. Nishijima, D. Ishida, K. Harada, T. Nabeshima, T. Sato, and T. Nakano, "A novel two-phase buck converter with two cores and four windings," in Proc. IEEE Int. Telecommun. Energy Conf., 2007, pp. 861–866.
- [9] K. I. Hwu and Y. T. Yau, "Active load for burn-in test of buck-type dc-dc converter with ultra-low output voltage," in Proc. IEEE Appl. Power Electron. Conf., 2008, pp. 635–638.
- [10] I. Laird and D. D. C. Lu, "High step-up dc/dc topology and MPPT algorithm for use with a thermoelectric generator," IEEE Trans. Power Electron., vol. 28, no. 7, pp. 3147–3157, Jul. 2013